

CuSO₄ nanoparticles loaded onto poly (toluenesulfonic acid-formaldehyde)/polyethyleneimine composites: An efficient retrievable catalyst for A₃/decarboxylative A₃ reactions

Wei Jiang¹ | Jinxi Xu¹ | Wei Sun¹ | Yiqun Li^{1,2}

¹Department of Chemistry, Jinan University, Guangzhou, 510632, China

²CAS Key Laboratory of Synthetic Chemistry of Natural Substances, Shanghai Institute of Organic Chemistry, Chinese Academy of Sciences, Shanghai, 200032, China

Correspondence

Yiqun Li, Department of Chemistry, Jinan University, Guangzhou 510632, China.
 Email: tlyq@jnu.edu.cn

Funding information

Natural Science Foundation of Guangdong Province, Grant/Award Number: 2020A1515010399

Using polymeric composite incorporated transition metal nanoparticles to promote various organic reactions has been found as one of the most powerful strategies in organic synthesis. In this paper, CuSO₄ nanoparticles (CuSO₄ NPs) anchored on the surface of polymeric composites comprising of water-insoluble acidic poly (toluenesulfonic acid-formaldehyde) (PTSAF) and water-soluble basic polyethyleneimine (PEI) to form the desired PEI/PTSAF-supported CuSO₄ NPs catalyst (CuSO₄NPs@PEI/PTSAF) have been fabricated. Characterization of the as-synthesized catalyst by inductively coupled plasma (ICP), Fourier transform infrared (FTIR), X-Ray diffraction (XRD), scanning electron microscopy (SEM), energy-dispersive spectroscopy (EDX) and elemental mapping analysis, transmission electron microscopy (TEM), and thermogravity analysis (TGA) demonstrated successful immobilization of the CuSO₄ NPs on the PEI/PTSAF composite. This novel catalyst was highly active in the one-pot A₃ and decarboxylative A₃ coupling reactions toward generating corresponding propargylamines in good to excellent yields under solvent-free reaction. The nature of the well distribution of CuSO₄ NPs coordinated with PEI ligand in the CuSO₄NPs@PEI/PTSAF composite leads to superior catalytic activity. The present methodology offers several advantages such as high catalytic activity, good to excellent yields, short reaction times, simple operations, compatibility of broad scope of substrates, and environmental friendliness. More importantly, the catalyst can be easily recovered from the reaction mixture by a simple filtration and still exhibits remarkable reusability with only marginal loss of its performance after five consecutive runs.

KEY WORDS

A₃ reaction, copper sulfate nanoparticles, decarboxylative A₃ reaction, poly (toluenesulfonic acid-formaldehyde), polyethyleneimine

Wei Jiang and Jinxi Xu contributed equally to this work.

1 | INTRODUCTION

Recently, great effort has been made to the transition metal-catalyzed one-pot multicomponent reaction of aldehyde, amine, and alkyne (commonly named A₃ reaction) as well as aldehyde/phenylglyoxylic acid, amine, and phenylpropionic acid (i.e., decarboxylative A₃ reaction) due to the main product propargylamine that is the key and versatile intermediate in the synthesis of many biologically active nitrogen-containing compounds.^[1] Therefore, it is necessary to explore an efficient homogeneous and heterogeneous catalysis to promote these three-component couplings. Despite of high activity of homogenous catalysis, some disadvantages such as moisture sensitivity, tedious isolation, and reuse of metal catalysts which severely contaminate the final product are frequently difficultly addressed. Moreover, aggregation and precipitation of the metal catalyst occur at times, which make the catalyst tend to lose its activity,^[2,3] while heterogeneous catalysis has salient features such as easy recovery and good recyclability. Therefore, heterogenization of homogenous catalyst on a suitable carrier is a more efficient way to tackle these obstacles of homogeneous catalysis which makes it practical for the synthesis of diversely molecules with pharmaceutical and biochemical applications in laboratorial and industrial scales.^[4–10] In order to achieve this purpose, heterogeneous catalysis has drawn much more focus. Among the heterogeneous catalysts, because copper catalysts are low cost, readily available, and high active, some heterogenized copper salts and its complexes were successfully used to catalyze A₃ and decarboxylative A₃ couplings. These reported heterogeneous copper catalysts include Cu^{II}@PAA/PVC mesoporous fibers,^[11] polymer beads decorated with dendrimer supported Cu (II),^[12] malachite,^[13] Cu⁰NPs@CMC,^[14] Fe₃O₄@SiO₂-Se-T/CuI,^[15] fiber-polyquaterniums@Cu(I),^[16] PS-PEG-BPy-CuBr₂,^[17] Cu⁰@HAP@γ-Fe₂O₃,^[18] chit@copper,^[19] polymer-supported copper (II) amine-imine complexes,^[20] Cu-MOF-74,^[21] Cu (II)-hydromagnesite,^[22] CMC-Cu^{II},^[23] Cu@PMO-IL,^[24] GO-CuCl₂,^[25] Cu⁰-Mont,^[26] CuSBA-15,^[27] Cu/Al/oxide mesoporous sponges,^[28] Cu-MOFs,^[29] Cu (OH) x-Fe₃O₄,^[30] copper thin films, and^[31] CuO NPs,^[32].

Generally, heterogenization is frequently achieved by immobilization of metal catalyst on both solid inorganic materials (SiO₂, Fe₃O₄, NaY, graphene, and carbon nanotube) and organic materials (polystyrene, polyethylene, PEG, etc.)^[4–6] which covalently tether the ligand. Although excellent catalytic performance has been achieved in some cases, most of ligand-functionalized heterogenous catalysts demonstrated decreased catalytic performance and selectivity

comparing with their catalyst parent. Moreover, multi-step synthetic approaches are necessary to achieve the ligand-functionalized support materials and significant structural perturbations to the parent metal catalyst are generally unavoidable in such circumstances. For the reason of practicality, simple and efficient alternative strategies that surmounted these obstacles for the immobilization of metal catalyst are therefore highly desirable. More recently, metal catalysts immobilized on ligand tethered to the support material via ionic bond have emerged as an attractive alternative with their powers being well-demonstrated in catalysis since complicated functionalization of the solid matrix is generally minimized. Moreover, the ionic bonding strategy is also quite facile, thus allowing fine tuning of the structure of support material, coordination of ligand, catalytic activity of catalyst parent, and their combination.^[33,34] Taking advantage of the ionic bonding principle, the solid acid/base interaction strategy has been proven to be one of the most efficient ionic bonding approaches for anchoring catalysts onto solid supports with excellent catalytic activity and reusability. To obtain uniform and homogenous dispersion of metal salt nanoparticles, many efforts have been made to develop base as a ligand utilized in designing of novel catalyst.

In recent years, introduction of polyethyleneimine (PEI) onto acidic solid materials has overwhelmingly impact on organometallic chemistry due to their unique properties. PEI is an amorphous, water-miscible branched polymer with repeating units of primary, secondary, and tertiary amine moieties.^[35,36] The PEI plays as a strong donor of electron pair and thus effectively enhances the electron density at the center of transit metal and thus accelerate the catalysis. Poly(toluenesulfonic acid-formaldehyde) (PTSAF) is a novel water-immiscible strong acidic resin synthesized by the copolymerization of *p*-toluenesulfonic acid and paraformaldehyde in the presence of catalytic amount of sulfuric acid.^[37] PTSAF is an inexpensive polymer possessing comparable acidity and cation exchange property. Thus, PEI can conveniently interact with PTSAF via a very strong ionic bonding interaction between acidic sulfonic groups and basic amino groups. Based on these properties of PEI and PTSAF, tethering of PEI ligands onto PTSAF material via ionic bond is particularly well suited for hosting metal salt nanoparticles for the following reasons: (1) the basic PEI can facilitate strong acid/base interaction with acidic PTSAF, (2) water-insoluble PTSAF serves as the vertebration, and water-soluble N-rich PEI providing the lone pair electrons as coordinating sites for chelation of transition metal species as the ligand, and (3) the catalytic transition metal species are coordinated by branched PEI chain and therefore fine

tuning their performance and preventing them leaching out from the support into solvent.

Although many works on A_3 and decarboxylative A_3 coupling reactions have been reported, as far as we observed, there have not reports using this PTSAF/PEI acid/base composite to immobilize the nanoparticles of transition metal salts and their catalytic application in A_3 and decarboxylative A_3 reactions. We envisage that the heterogenization of transition metal salts on this type of composite by combination of “two worlds” of distinct acidic and basic polymers is a powerful strategy to accelerate organic reactions efficiently in one-pot catalysis. Herein, we have developed an efficient protocol for integration of acidic PTSAF as a support and basic PEI as a ligand to support $CuSO_4$ NPs for the fabrication of a highly active catalyst for A_3 and decarboxylative A_3 reaction (Figure 1).

2 | EXPERIMENTAL

2.1 | General considerations

All chemicals and solvents were analytical grade and used as received. Scanning electron microscopy (SEM) and energy-dispersive spectroscopy (EDX) were conducted with a Zeiss Sigma 500 instrument. X-ray photoelectron spectroscopy (XPS) was carried out on a Thermo Fisher Scientific K-Alpha instrument. X-Ray diffraction (XRD) was performed on a Bruker D8. Thermogravimetric analysis (TGA) was performed on a Netzsch STA449 under a nitrogen atmosphere from 30°C to 800°C in a 50 ml min⁻¹ N₂ flow and a ramp rate of 10°C min⁻¹. The elemental copper content of the catalyst was determined by inductively coupled plasma atomic emission spectrometry (ICP-AES) using X Series 2 instrument. Gas chromatography (GC) was performed on a Shimadzu GCMS-QP2020. Fourier transform infrared spectra (FTIR) were collected on a Nicolet 6700 spectrophotometer in KBr pellet within the spectral range of 4,000–400 cm⁻¹ at 2 cm⁻¹ resolution and 32 scans. ¹H NMR and ¹³C NMR spectra were recorded on a Bruker-300 Avance Spectrometer with CDCl₃ as solvent using TMS as an internal standard at 300 and 75 MHz, respectively.

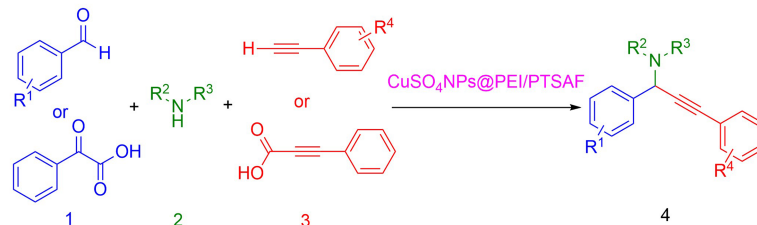
2.2 | Preparation of CuSO₄NPs@PEI/PTS AF catalyst

Initially, the mixture of *p*-toluenesulfonic acid (10 g), paraformaldehyde (2 g), and sulfuric acid (0.2 g) was heated at 110°C with constant stirring for 48 h to form black solid. The resulted black solid (named PTSAF) was filtered and washed thoroughly with deionized water until the filtrate reached neutral. Subsequently, the obtained PTSAF was dried at 120°C in an oven overnight. Next, the grinded PTSAF powders were soaked in 20 ml of 50% PEI solution at room temperature for 48 h and then filtered and washed with a plenty of deionized water in order to remove excess PEI from the PTSAF surface. Furthermore, the as-prepared PEI/PTS AF composite material was immersed into 200 ml 0.1 mol/L sodium carbonate solution for 12 h. After that, the treated PEI/PTS AF materials were washed thoroughly with deionized water and ethanol then dried at 60°C till a constant weight. Finally, PEI/PTS AF black power (1 g) was soaked in the already-prepared 100 ml 2% CuSO₄ solution and gently agitated at room temperature for 24 h. The obtained CuSO₄NPs@PEI/PTS AF catalyst was filtered out and washed repeatedly with deionized water and then dried at 40°C to constant weight. The Cu content in catalyst determined by ICP is 0.6575 mmol/g.

2.3 | General procedure for the A_3 and decarboxylative A_3 reactions

Aldehyde/phenylglyoxylic acid (1.0 mmol), amine (1.2 mmol), terminal alkyne/phenylpropionic acid (1.5 mmol), and catalytic amount of CuSO₄NPs@PEI/PTS AF (1.5 mol% Cu) were charged into a sealed vessel. The mixture was stirred at 100°C for specific time indicated by thin-layer chromatography (TLC) to the end of reaction. The CuSO₄NPs@PEI/PTS AF was filtered and washed with enough AcOEt (15 ml × 3), and the organic phase was combined and washed with brine (5 ml × 3) and dried over anhydrous Na₂SO₄. Then the solvent was evaporated in vacuum, and the residue was purified by preparative thin-layer chromatography (PTLC) to afford the corresponding propargylamine.

FIGURE 1 CuSO₄NPs@PEI/PTS AF-catalyzed the A_3 and decarboxylative A_3 for the synthesis of propargylamines



3 | RESULTS AND DISCUSSION

3.1 | Preparation and characterization of catalyst

Firstly, we adopted a facile method to prepare an insoluble acidic PTSAF by copolymerization of toluenesulfonic acid and formaldehyde according to previous reported procedures.^[37] Subsequently, the water-soluble basic PEI was grafted onto PTSAF matrix via ionic bond by acid/base reaction. Finally, CuSO₄NPs@PEI/PTS AF catalysts were synthesized by the treatment of CuSO₄ solution with PEI/PTS AF composite materials. The synthetic routes have been outlined in Scheme 1.

The obtained CuSO₄NPs@PEI/PTS AF catalyst was fully characterized with various analysis techniques such as inductively coupled plasma (ICP), FTIR spectroscopy, XRD, SEM, energy dispersive X-ray (EDX) mapping analysis, transmission electron microscopy (TEM), and thermogravimetry analysis (TGA).

The FTIR spectra of PEI/PTS AF and CuSO₄NPs@PEI/PTS AF are shown in Figure 2. As shown in Figure 2, the stretching peak at 3,427 cm⁻¹ together with bending peak at 1,454 cm⁻¹ (curve a) is attributed to

characteristic N-H.^[36,38,39] When CuSO₄ immobilized on PTSAF, the electron cloud density of the nitrogen atoms on PEI of the PEI/PTS AF decreases, and the N-H absorption peaks move to lower wave number from 1,454 to 1,443 cm⁻¹ (curve b), respectively.

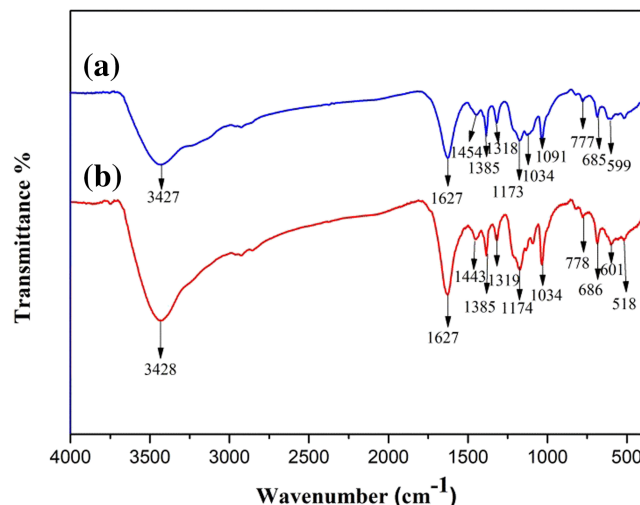
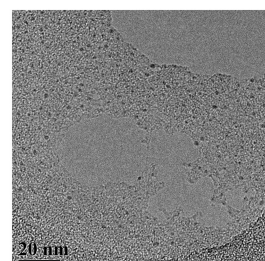
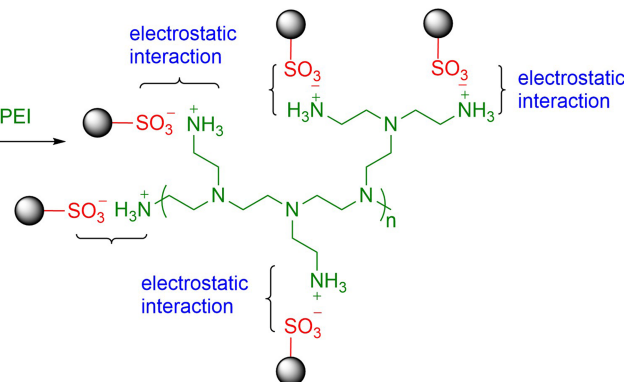
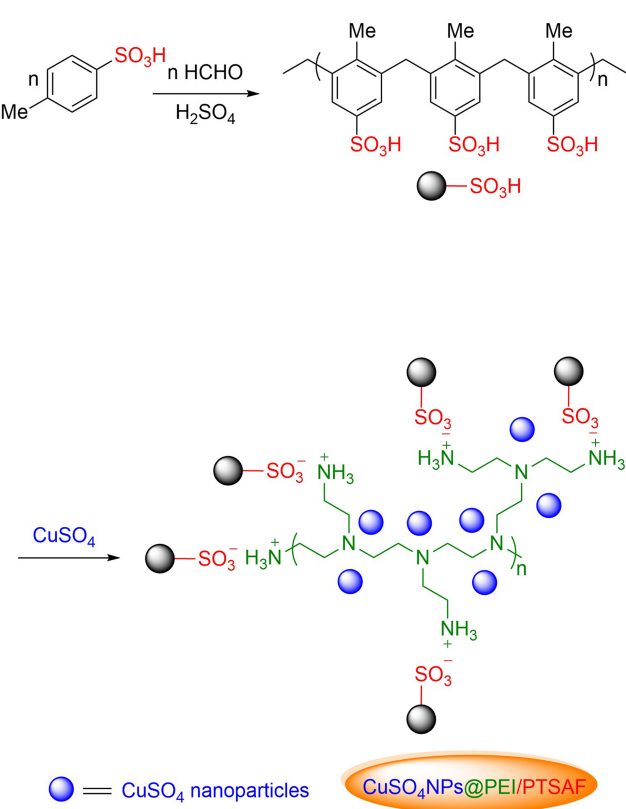


FIGURE 2 Fourier transform infrared (FTIR) spectra of polyethylenimine (PEI)/poly (toluenesulfonic acid-formaldehyde) (PTS AF) (a) and CuSO₄NPs@PEI/PTS AF (b)



SCHEME 1 Schematic process for preparation of CuSO₄NPs@PEI/PTS AF catalyst

The XRD patterns of PTSAF (curve a), PTSAF/PEI (curve b), CuSO₄NPs@PEI/PTS AF (curve c), and CuSO₄·5H₂O (curve d) are shown in Figure 3. One broad peak ($2\theta = 19^\circ$) is present in PTSAF, PTSAF/PEI, and CuSO₄NPs@PEI/PTS AF, respectively. By comparison with CuSO₄·5H₂O (curve d), no diffraction peaks of CuSO₄·5H₂O were found in these samples. This fact may be due to the very small size and nanocrystalline nature of the CuSO₄ with lower weight percentage or high dispersion in amorphous nanoform in catalyst structure.

The XPS was used to confirm the oxidation state of elements presented in the as-synthesized catalyst. The full spectra and fitting curves of high-resolution spectra are presented in Figure 4. The survey profiles for Cu_{2p}, S_{2p}, O_{1s}, N_{1s}, and C_{1s} of the CuSO₄NPs@PEI/PTS AF are plotted in Figure 4(a). The Cu_{2p} peak shown in Figure 4(b) shows four components at 962.5, 953.4, 942.7, and 933.7 eV which can be attributed to Cu (II) in CuSO₄.^[40,41] The sulfur peaks shown in Figure 4(c) contain two components at 169.2 and 167.8 eV which match the reported values of the binding energies of sulfur from CuSO₄ and CuSO₃.^[42,43] The peaks at 286.6 and 284.9 eV in Figure 4(d) were assigned to the C–N and C–C bonds in PEI. The binding energies at 401.8 and 399.8 eV in Figure 4(e) were attributed to the N–H bond in –NH₃⁺ and –NH₂ groups of PEI, correspondingly. These results suggest that CuSO₄ were successfully loaded on the PEI/PTS AF surface.

The SEM images of CuSO₄NPs@PEI/PTS AF shown in Figure 5 were recorded at low (2 μm) and high magnifications (100 nm) for easy clarity and comparison. The rough surface can be observed for CuSO₄NPs@PEI/PTS AF catalyst in Figure 5(a)–5(d). The rough surface of

the catalyst facilitates better mass transfer and enlarges its interaction area with reaction substrates.

The SEM images and corresponding elemental maps for the prepared CuSO₄NPs@PEI/PTS AF catalyst are presented in Figure 6. These images clearly showed that the C, O, N, S, and Cu elements were finely dispersed throughout the catalyst in a homogeneous manner. These results demonstrated that CuSO₄ was immobilized on the PEI/PTS AF surface.

The EDX analysis provides local elemental information for the catalyst. The EDX of the CuSO₄NPs@PEI/PTS AF associated with SEM analysis is shown in Figure 7. The EDX indicated that the obtained catalyst was composed of nonmetallic elements N, O, and S, and metallic element Cu. The observation of Cu and S element in EDX analysis proved the successful introduction of CuSO₄ on PEI/PTS AF surface.

In order to have an insight into the morphology of the catalyst, the TEM images of CuSO₄NPs@PEI/PTS AF were recorded varied from 10 nm to 1 μm (Figure 8), showing the formation of quasi-spherical nanoparticles (Figure 8(a)). The particle size histogram (Figure 8(f)) shows that the average particle size of CuSO₄ located in the catalyst is approximately 1.21 nm in diameter, respectively.

The TGA was conducted in nitrogen atmosphere varying from 25°C to 800°C. As can be seen from the plot in Figure 9, there are two-step thermal decomposition. The incipient weight loss laid in the range of 25°C to 100°C was attributed to the removal of loosely physically adsorbed water. Then the main weight loss in the range of 275°C to 500°C is assigned to the decomposition of PEI and PTS AF. In addition, the plot presented higher ash content, which attributed to the copper residue. The TGA results indicated that CuSO₄NPs@PEI/PTS AF is sufficiently stable from room temperature to 250°C and thus can be performed under our thermal conditions.

3.2 | Performance of catalyst for the A₃ and decarboxylative A₃ reactions

To evaluate the catalytic activity of CuSO₄NPs@PEI/PTS AF, the reaction of benzaldehyde (**1a**), morpholine (**2a**), and phenylacetylene (**3a**) was chosen as a model. The reaction temperatures, various solvents, and different loading of catalyst were symmetrically investigated. The results are listed in Table 1. In order to establish the CuSO₄ NPs in the catalyst plays the key role in the reaction, the model reaction was performed at 100°C in the absence of catalyst, and in the presence of 1.5 mol% of PTS AF, PEI, PEI/PTS AF, Cu^{II}@PTS AF, PEI-CuSO₄ and CuSO₄NPs@PEI/PTS AF under solvent-free condition,

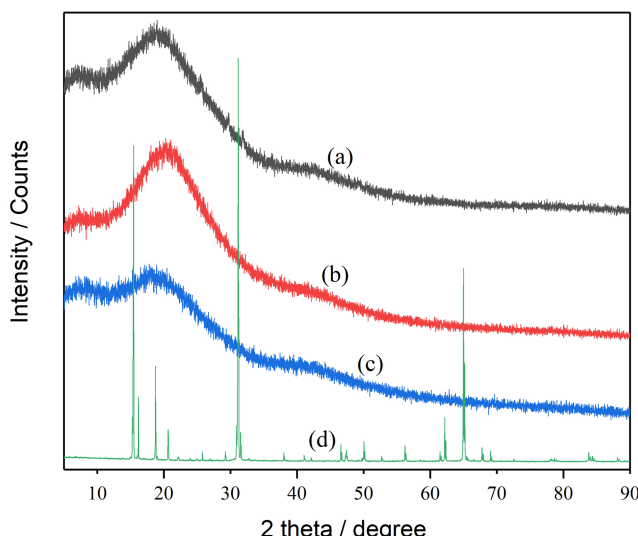


FIGURE 3 X-Ray diffraction (XRD) of PTSAF (a), PEI/PTS AF (b), CuSO₄NPs@PEI/PTS AF (c), and CuSO₄·5H₂O (d)

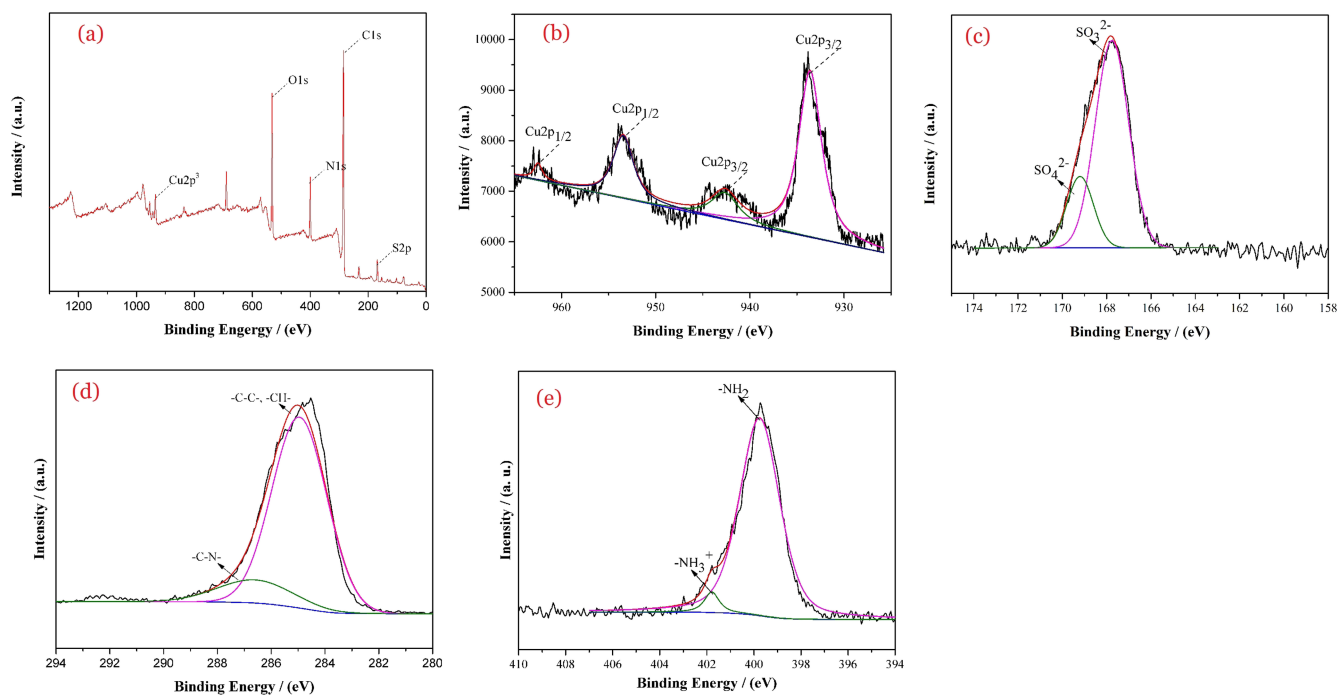


FIGURE 4 The X-ray photoelectron spectroscopy (XPS) and spectra scan of element survey (a), Cu_{2p} (b), S_{2p} (c), C_{1s} (d), and N_{1s} (e)

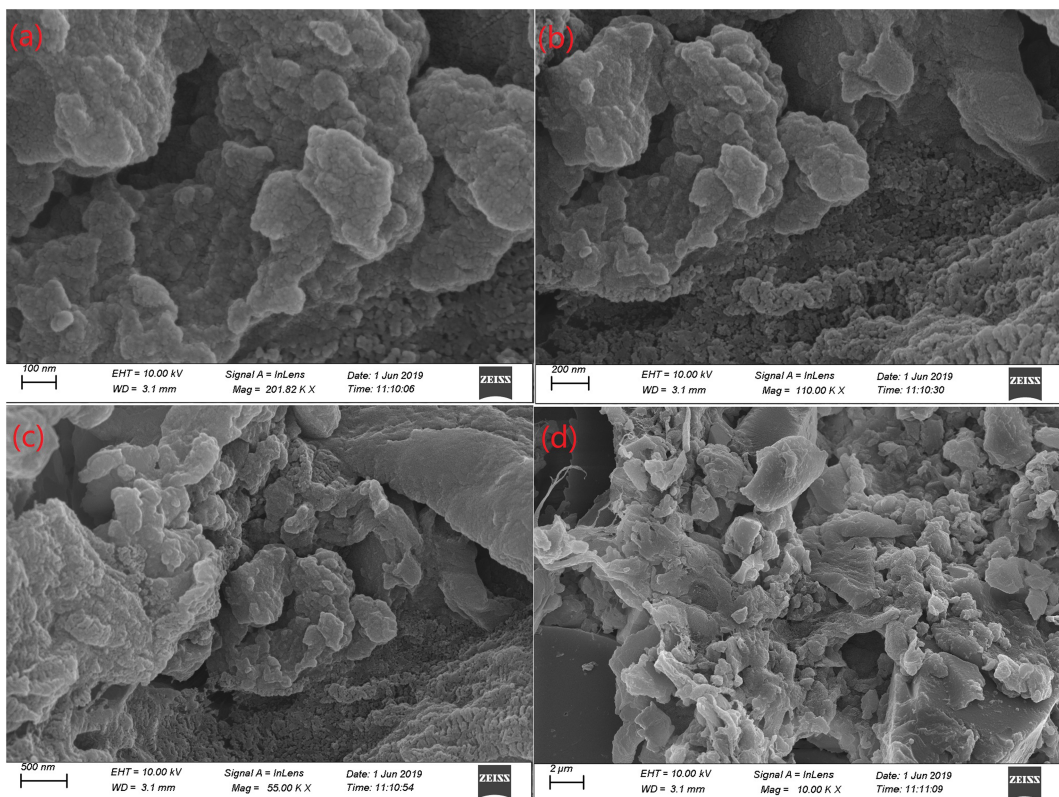


FIGURE 5 The scanning electron microscopy (SEM) imagines of CuSO₄NPs@PEI/PTS AF (a in 100 nm, b in 200 nm, c in 500 nm, and d in 2 μm)

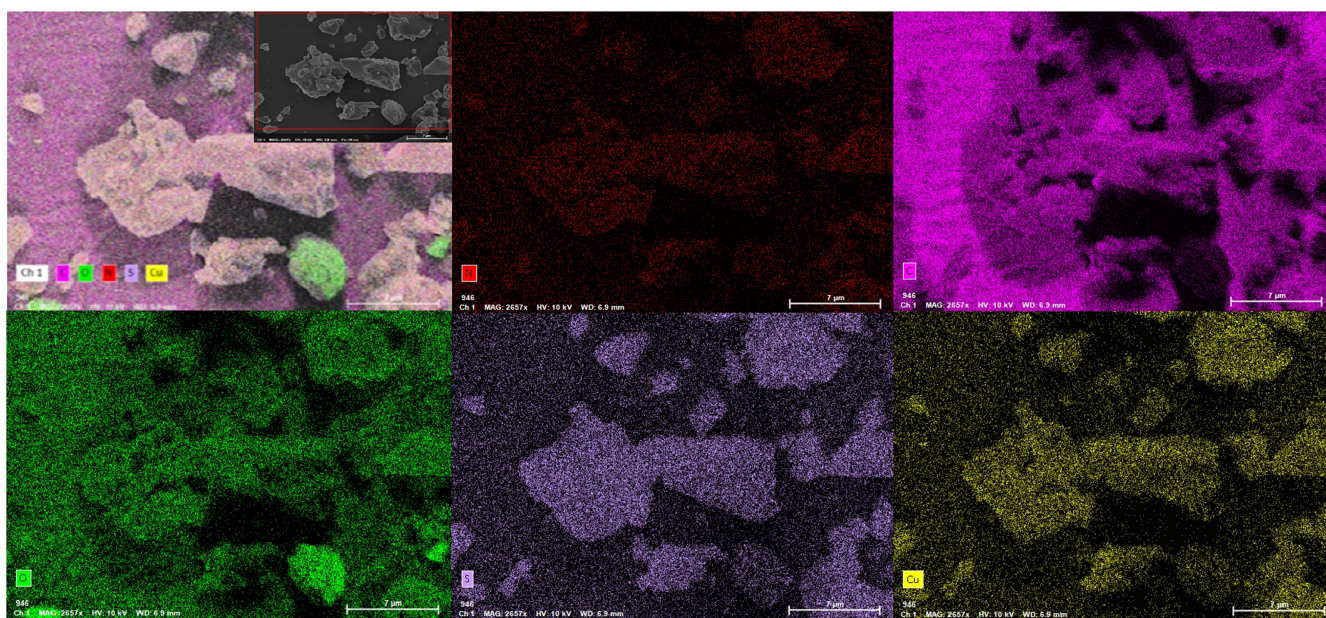
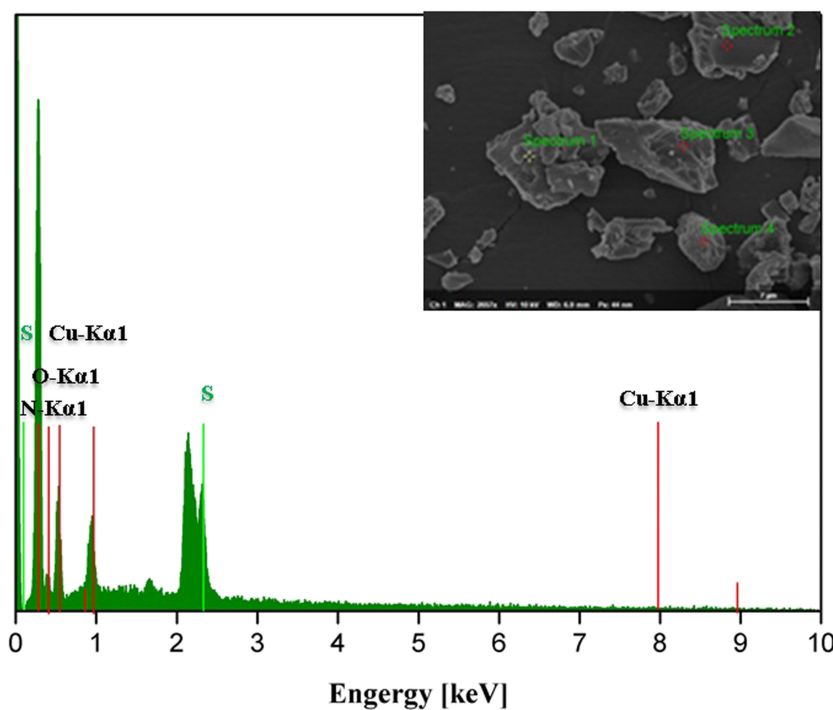


FIGURE 6 The scanning electron microscopy (SEM) mapping imagines of $\text{CuSO}_4\text{NPs@PEI/PTSAF}$ show the presence of C, N, O, S, Cu element in the catalyst

FIGURE 7 Energy-dispersive spectroscopy (EDX) element analysis of $\text{CuSO}_4\text{NPs@PEI/PTSAF}$



the product yields ranged from 0% and up to 90% (Table 1, entries 2–8). Further increasing the dose of catalyst from 1.5 to 2 even up to 3 mol%, no significant elevation in the reaction yield was observed (Table 1, entries 9–10). On the other hand, decreasing the amount of catalyst reduced the yield of the product (Table 1, entries 11–13). These results suggested that the catalyst is

essential for this A_3 model reaction and the catalytically active species is Cu (II), and 1.5 mol % of Cu is the optimal amount for the model reaction. Then the temperature effect on the model was investigated. Increasing the temperature from 100°C to 120°C has no apparent impact on the product yields (Table 1, entries 14–15). On the contrary, decreasing the reaction temperature from

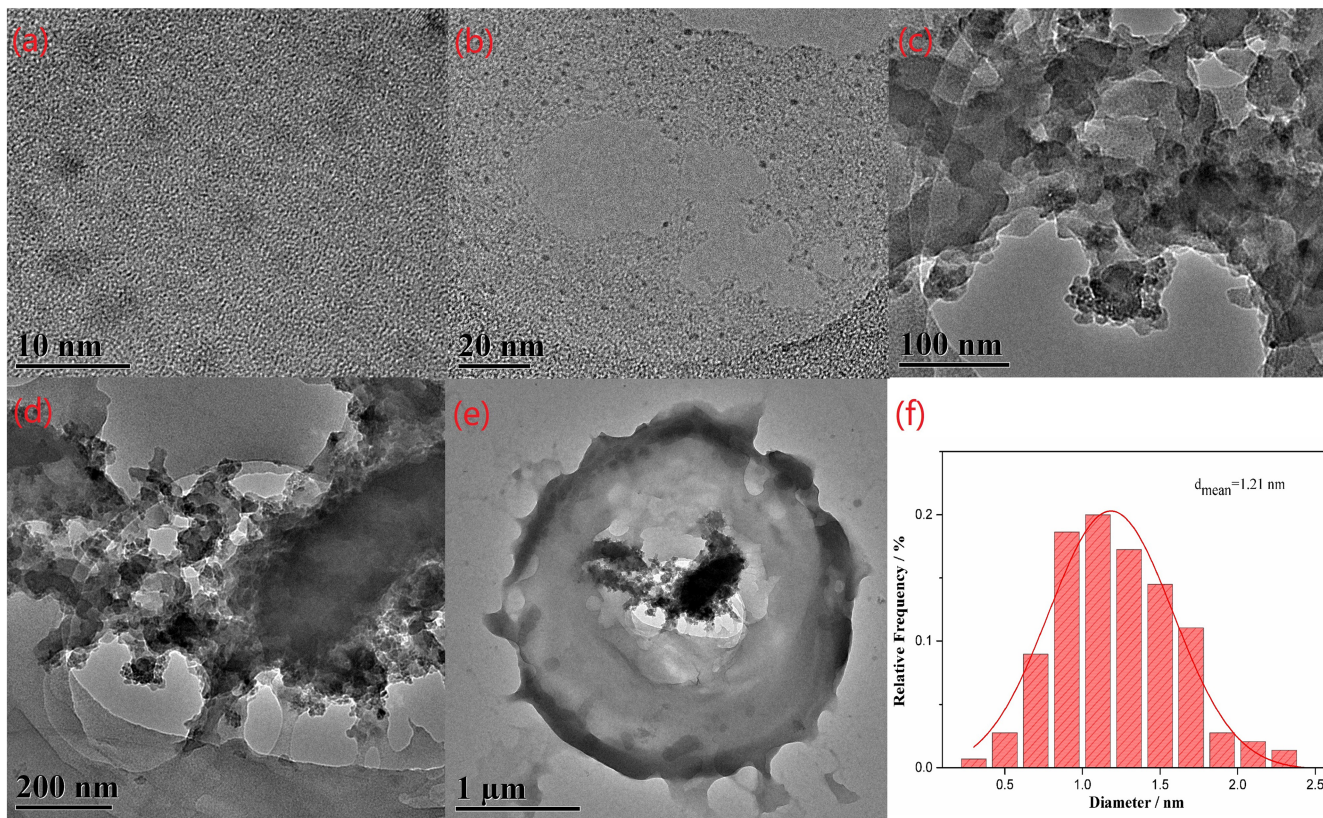


FIGURE 8 The transmission electron microscopy (TEM) images of CuSO₄NPs@PEI/PTSAF (a in 10 nm, b in 20 nm, c in 100 nm, d in 200 nm, and e in 1 μ m) and the diameter analysis of CuSO₄NPs (f) calculation based on image (b)

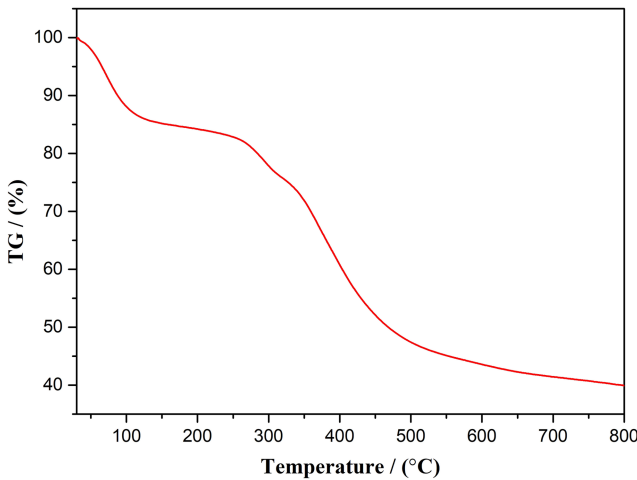
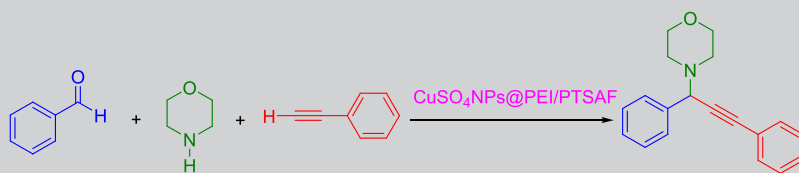


FIGURE 9 The thermogravimetry analysis (TGA) curves of CuSO₄NPs@PEI/PTSAF

100°C to room temperature had considerable negative influence on the model reaction (Table 1, entries 16–18). The effect of the solvent was also examined. The model reaction was carried out under solvent-free condition as well as in the different solvents such as toluene, THF,

EtOH, CH₃CN, DMF, and DMSO (Table 1, entries 1 and 19–24). Gratifyingly, the highest yields were obtained when the reaction was conducted under the neat condition and in toluene. From the viewpoint of green chemistry, we will conduct the A₃ and decarboxylative A₃ reactions in the succeeding work under the solvent-free condition.

With the optimal condition in hand, the scope of the reactions using various carbonyl compounds/phenylglyoxylic acids, amines, and alkynes/phenylpropionic acids was explored, and the results are summarized in Table 2. In the cases of A₃ coupling, aryl aldehydes with electron-withdrawing or electron-donating substituents afforded moderate to excellent yields when it reacted with morpholine and phenylacetylene (Table 2, entries 1–9). The heterocyclic 2-thiophene formaldehyde with morpholine and phenylacetylene also underwent efficiently and afford the corresponding product in excellent yield (Table 2, entry 10). Interestingly, the reaction between aliphatic aldehyde and morpholine with phenylacetylene formed the desired product in good yields due to their higher reactivity (Table 2, entry 11). Notably, the phenylacetylene bearing either electron-donating or electron-withdrawing groups on the aromatic

TABLE 1 Optimization of reaction conditions

| Entry | Solvent | Temp. (°C) | Catalyst (mol%) | Time (h) | Yield ^a (%) |
|-------|----------------------------------|------------|--|----------|------------------------|
| 1 | Solvent-free | 100 | none | 4 | N.P. ^b |
| 2 | Solvent-free | 100 | PTSAF/PEI (1.5) | 4 | N.P. |
| 3 | Solvent-free | 100 | PEI (1.5) | 4 | N.P. |
| 4 | Solvent-free | 100 | PTSAF (1.5) | 4 | N.P. |
| 5 | Solvent-free | 100 | CuSO ₄ ·5H ₂ O (1.5) | 8 | 66 |
| 6 | Solvent-free | 100 | Cu ^{II} @PTSAF (1.5) | 4 | 56 |
| 7 | Solvent-free | 100 | PEI-CuSO ₄ (1.5) | 6 | 22 |
| 8 | Solvent-free | 100 | CuSO ₄ NPs@PEI/PTSAF (1.5) | 4 | 92 |
| 9 | Solvent-free | 100 | CuSO ₄ NPs@PEI/PTSAF (2.0) | 4 | 93 |
| 10 | Solvent-free | 100 | CuSO ₄ NPs@PEI/PTSAF (3.0) | 4 | 96 |
| 11 | Solvent-free | 100 | CuSO ₄ NPs@PEI/PTSAF (1.2) | 4 | 86 |
| 12 | Solvent-free | 100 | CuSO ₄ NPs@PEI/PTSAF (0.8) | 4 | 84 |
| 13 | Solvent-free | 100 | CuSO ₄ NPs@PEI/PTSAF (0.4) | 4 | 73 |
| 14 | Solvent-free | 110 | CuSO ₄ NPs@PEI/PTSAF (1.5) | 4 | 91 |
| 15 | Solvent-free | 120 | CuSO ₄ NPs@PEI/PTSAF (1.5) | 12 | 96 |
| 16 | Solvent-free | 80 | CuSO ₄ NPs@PEI/PTSAF (1.5) | 12 | 17 |
| 17 | Solvent-free | 60 | CuSO ₄ NPs@PEI/PTSAF (1.5) | 12 | Trace |
| 18 | Solvent-free | r.t. | CuSO ₄ NPs@PEI/PTSAF (1.5) | 12 | N.P. |
| 19 | Toluene | 120 | CuSO ₄ NPs@PEI/PTSAF (1.5) | 12 | 92 |
| 20 | THF | 80 | CuSO ₄ NPs@PEI/PTSAF (1.5) | 12 | 46 |
| 21 | C ₂ H ₅ OH | 80 | CuSO ₄ NPs@PEI/PTSAF (1.5) | 12 | 27 |
| 22 | CH ₃ CN | 80 | CuSO ₄ NPs@PEI/PTSAF (1.5) | 12 | 27 |
| 23 | DMF | 120 | CuSO ₄ NPs@PEI/PTSAF (1.5) | 12 | 44 |
| 24 | DMSO | 120 | CuSO ₄ NPs@PEI/PTSAF (1.5) | 12 | 62 |

Note: Reaction conditions: benzaldehyde (1.0 mmol), morpholine (1.2 mmol), phenylacetylene (1.5 mmol), catalytic amount of catalyst in a sealed vial.

^aIsolated yields.

^bN.P. refers to no product.

ring are readily coupled with carbonyl compounds and amines in moderate to excellent yields (Table 2, entries 14–16 and 20–21). Various amines also proceeded smoothly in A₃ coupling reaction and generated the corresponding products in good to excellent yields. Among the amines, alicyclic amine such as morpholine gave good yields of corresponding products, whereas moderate yields were observed as acyclic dialkylamines

were used (Table 2, entries 17–18). These successful results encouraged us to extend the present catalytic approach to a wide variety of substrates. Then we turned our attention toward decarboxylative A₃ reaction. We further expanded the substrates to phenylglyoxylic acids as aldehyde sources and phenylpropionic acid as a phenylacetylene surrogate. The substrate of phenylglyoxylic acids and

TABLE 2 CuSO₄NPs@PEI/PTSAF-catalyzed synthesizing of propargylamines through A₃ reaction

| Entry | Aldehyde | Amine | Alkyne | Time (h) | Product | Yield ^a (%) |
|-------|----------|-------|--------|----------|-----------|------------------------|
| 1 | | | | 6 | 4a | 96 |
| 2 | | | | 6 | 4b | 87 |
| 3 | | | | 6 | 4c | 97 |
| 4 | | | | 6 | 4d | 85 |
| 5 | | | | 6 | 4e | 94 |
| 6 | | | | 6 | 4f | 62 |
| 7 | | | | 6 | 4g | 80 |

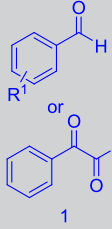
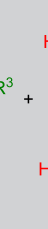
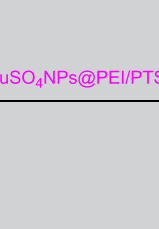
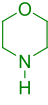
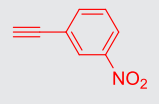
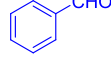
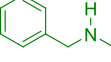
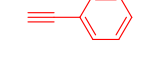
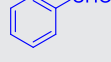
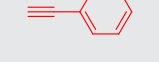
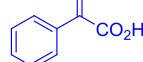
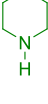
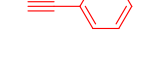
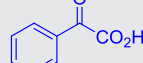
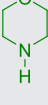
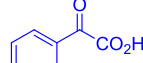
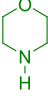
(Continues)

TABLE 2 (Continued)

| Entry | Aldehyde | Amine | Alkyne | Time (h) | Product | Yield ^a (%) |
|-------|----------|-------|--------|----------|-----------|------------------------|
| | | | | | 1 | 2 |
| 8 | | | | 6 | 4h | 92 |
| 9 | | | | 6 | 4i | 83 |
| 10 | | | | 6 | 4j | 85 |
| 11 | | | | 4 | 4k | 99 |
| 12 | | | | 4 | 4l | 99 |
| 13 | | | | 4 | 4m | 85 |
| 14 | | | | 4 | 4n | 84 |

(Continues)

TABLE 2 (Continued)

| Entry | Aldehyde | Amine | Alkyne | Time (h) | Product | | Yield ^a (%) |
|-------|---|---|---|----------|-----------|--|------------------------|
| | | | | | | | |
| 15 |  |  |  | 4 | 4o | | 80 |
| 16 |  |  |  | 4 | 4p | | 83 |
| 17 |  |  |  | 4 | 4q | | 92 |
| 18 |  |  |  | 4 | 4r | | 86 |
| 19 |  |  |  | 12 | 4a | | 68 |
| 20 |  |  |  | 12 | 4l | | 74 |
| 21 |  |  |  | 12 | 4n | | 72 |

(Continues)

TABLE 2 (Continued)

| Entry | Aldehyde | Amine | Alkyne | Time (h) | Product | Yield ^a (%) |
|-------|----------|-------|--------|----------|-----------|------------------------|
| | | | | | 1 | 2 |
| 22 | | | | 12 | 4a | 60 |
| 23 | | | | 12 | 4b | 63 |
| 24 | | | | 12 | 4f | 80 |

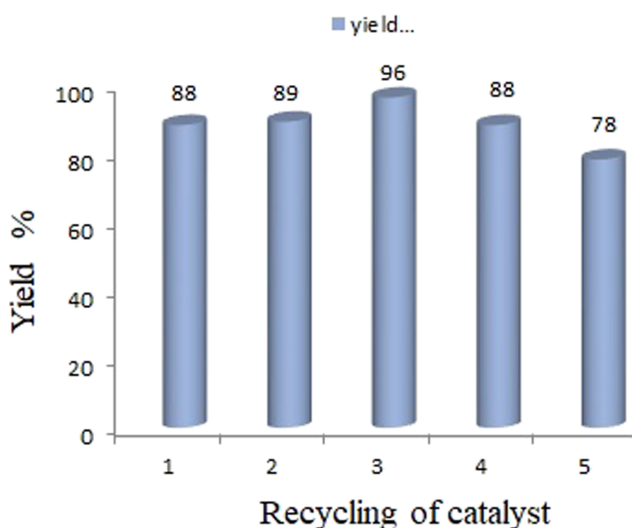
Note: Reaction conditions: aldehyde/phenylglyoxylic acid (1.0 mmol), amine (1.2 mmol), alkyne/phenylpropionic acid (1.5 mmol), CuSO₄NPs@PEI/PTSAF (1.5 mol %), solvent-free, 4–12 h, 100°C.

^aIsolated yields.

phenylpropionic acid reacted well under the optimal condition to afford the corresponding products in excellent yields (Table 2, entries 19–24).

3.3 | Recycling of catalyst for the A₃ model reaction

In order to clarify the reusabilities of CuSO₄NPs@PEI/PTSAF catalyst in A₃ couplings, the model reaction of *p*-chlorobenzaldehyde, morpholine, and phenylacetylene was evaluated under the optimal reaction condition. Upon the completion of the reaction, the CuSO₄NPs@PEI/PTSAF catalyst was recollected conveniently by filtration and reused directly in the subsequent run without any further treatment. The results as shown in Figure 10 indicated that the CuSO₄NPs@PEI/PTSAF

**FIGURE 10** Recycling of catalyst in the A₃ model reaction

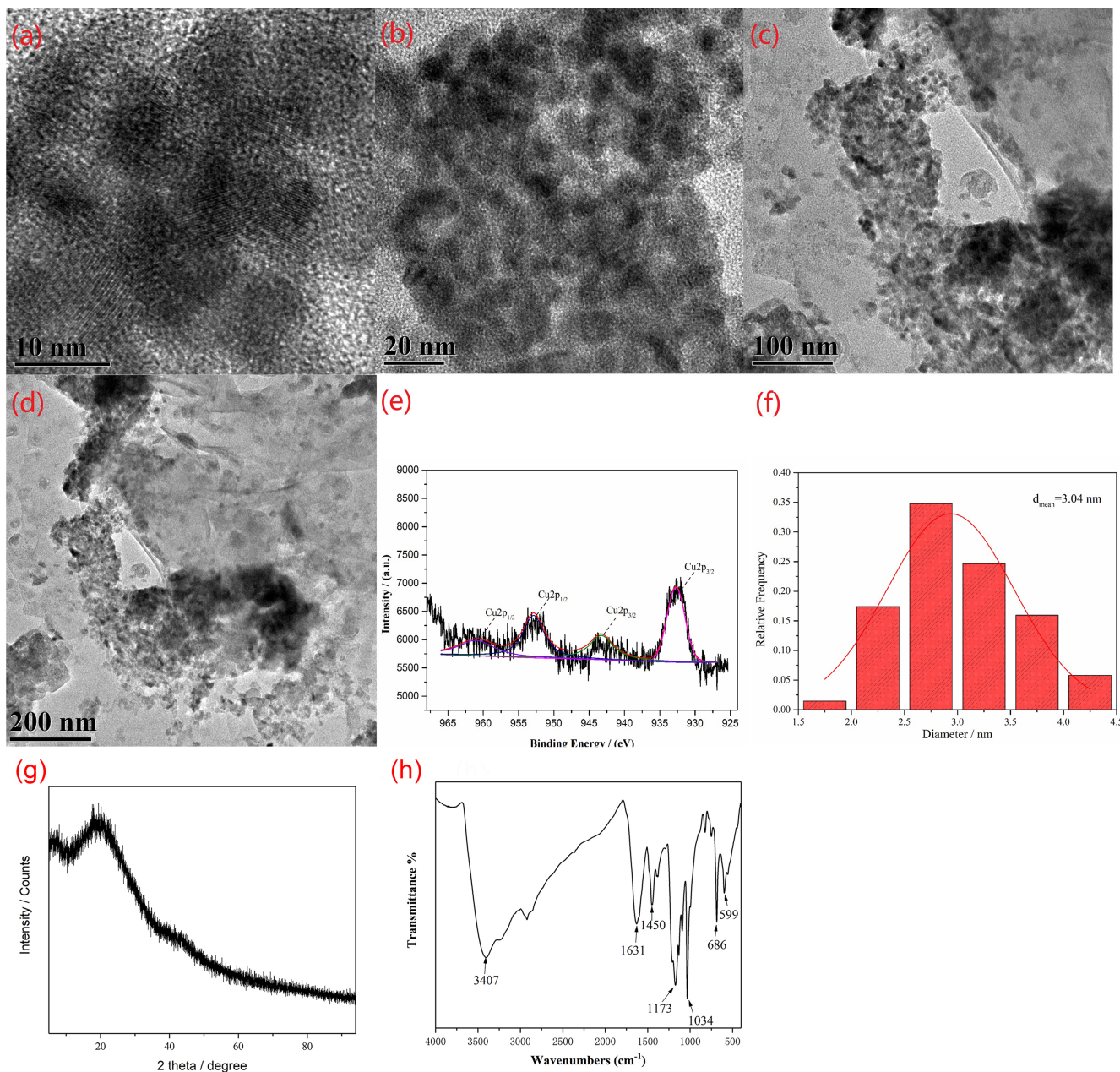


FIGURE 11 The transmission electron microscopy (TEM) images of the used catalyst at different magnification (a–d), the X-ray photoelectron spectroscopy (XPS) of the used catalyst (e), the diameter analysis of used catalyst based on image b (f), the X-Ray diffraction (XRD) pattern of the used catalyst (g), and Fourier transform infrared (FTIR) of used catalyst (h)

catalyst can be used for at least five consecutive runs successfully with slight decreasing its catalytic performance.

Furthermore, the XPS, TEM, XRD, and FTIR (Figure 11) of the recovered catalyst after five runs show that the morphology, chemical, and oxidation state of the catalyst have no significant changes and the particle sizes slightly increased from 1.21 to 3.04 nm in diameter. These findings indicated that the catalyst was intact after multiple reusages. These findings not only explained the excellent recycle results but also furtherly confirmed the excellent stability of this composite catalyst.

3.4 | Comparison with other reported copper catalysts

Finally, to demonstrate the worthiness and efficiency of the CuSO₄NPs@PEI/PTS AF catalyst in the synthesis of propargylamine derivatives, it has been compared with other previously published copper catalysts using the A₃ model reaction. The comparative results presented in Table 3 clearly demonstrate that the present catalyst indeed has superior catalytic performance in terms of low catalyst loading, short reaction time, and excellent yield.

TABLE 3 Comparison of the present catalyst with previous reported copper catalysts in A₃ model reaction

| Entry | Catalyst (dose) | Reaction conditions | Yield (%) | Ref |
|-------|---|--|-----------|-----------|
| 1 | polymer beads decorated with dendrimer supported Cu (II) (1 mol%) | 1,4-dioxane, 90°C, 9 h | 87 | [12] |
| 2 | Cu ⁰ NPs@CMC (7.5 mol%) | Neat, 120°C, 12 h | 80 | [14] |
| 3 | fiber-polyquaterniums@Cu(I) (2 mol%) | Toluene, 100°C, 6 h | 94 | [16] |
| 4 | chit@CuI (1.1 mol%) | Neat, 140°C, under N ₂ , 0.75 h | 83 | [19] |
| 5 | polymer-supported copper (II) mine-imine complexes (1 mol%) | 1,4-dioxane, 80°C, 24 h | 91 | [20] |
| 6 | CMC-Cu ^{II} (5 mol%) | Neat, 120°C, 15 h | 81 | [23] |
| 7 | Cu/Al/oxide mesoporous sponges (12 mol%) | Toluene, 100°C, 22 h | 94 | [28] |
| 8 | CuO NPs (8 mol%) | Toluene, 90°C, 7 h | 80 | [32] |
| 9 | CuSO ₄ NPs@PEI/PTSAF | Neat, 100°C, 6 h | 96 | This work |

In addition, solvent-free condition and easy separation and recycling of catalyst are some obvious benefits with respect to the other methods.

4 | CONCLUSIONS

In this work, we fabricated a novel and retrievable catalyst with architecture of CuSO₄ NPs loaded onto the PEI/PTSAF composite materials for the synthesis of propargylamine via A₃ and decarboxylative A₃ reactions in excellent yields under solvent-free condition. The as-synthesized composite catalyst is fully characterized by FTIR, XPS, SEM, EDX, TEM, and TGA techniques. The experimental results have demonstrated that the CuSO₄NPs@PEI/PTSAF catalyst exerts high catalytic performance for A₃ and decarboxylative A₃ reaction. The high catalytic activity can be attributed to the unique inherent property of CuSO₄ NPs fine-tuned by PEI via coordination. High catalytic activity, low cost, simple isolation, short reaction time, mild condition, recycling of catalyst, and tolerance of wide scope of substrates are the salient features of this green catalytic process. Moreover, the catalyst can be easily separated by suction and reused at least five consecutive runs with a slight loss of catalytic activity.

DATA AVAILABILITY STATEMENT

The data that support the findings of this study are available in the supporting information of this article.

ACKNOWLEDGMENTS

We are grateful to the Natural Science Foundation of Guangdong Province (2020A1515010399) for financial support.

CONFLICT OF INTEREST

The authors declare no competing financial interest.

REFERENCES

- [1] K. Lauder, A. Toscani, N. Scalacci, D. Castagnolo, *Chem. Rev.* **2017**, *117*, 14091.
- [2] D. Astruc, *Inorg. Chem.* **2007**, *46*, 1884.
- [3] I. Beletskaya, V. Tyurin, *Molecules* **2010**, *15*, 4792.
- [4] B. C. Ranu, S. Bhadra, D. Saha, *Curr. Org. Synth.* **2011**, *8*, 146.
- [5] A. Bahuguna, A. Kumar, V. Krishnan, *Asian J. Org. Chem.* **2019**, *8*, 1263.
- [6] M. Benaglia, A. Puglisi, F. Cozzi, *Chem. Rev.* **2003**, *103*, 3401.
- [7] J. Safaei-Ghom, Z. Omidshafiei, *RSC Adv.* **2019**, *9*, 37344.
- [8] J. Safaei-Ghom, F.-S. Bateni, P. Babaei, *Appl. Organomet. Chem.* **2020**, *34*, e5657.
- [9] J. Safaei-Ghom, S. H. Nazemzadeh, H. Shahbazi-Alavi, *Appl. Organomet. Chem.* **2016**, *30*, 911.
- [10] S. Barkhordarion-Mohammadi, J. Safaei-Ghom, *Z. Naturforsch.* **2018**, *73*, 17.
- [11] W. Jiang, Y. Zhou, W. Sun, Y. Li, *Appl. Organomet. Chem.* **2020**, *34*, e5429.
- [12] A. Bukowska, K. Bester, M. Pytel, W. Bukowski, *Catal. Lett.* **2020**. <https://doi.org/10.1007/s10562-020-03301-0>
- [13] M. Milen, G. Györke, A. Dancsó, B. Volk, *Tetrahedron Lett.* **2020**, *61*, 151544.
- [14] X. Liu, X. Tan, Y. Zhou, Y. Li, Z. Zhang, *Res. Chem. Intermed.* **2019**, *45*, 3359.
- [15] Y. Rangraz, F. Nemati, A. Elhampour, *Ind. Eng. Chem. Res.* **2019**, *58*, 17308.
- [16] Q. Hu, X.-L. Shi, Y. Chen, F. Wang, Y. Weng, P. Duan, *J. Ind. Eng. Chem.* **2019**, *69*, 387.
- [17] S. Yan, S. Pan, T. Osako, Y. Uozumi, *ACS Sustainable Chem. Eng.* **2019**, *7*, 9097.
- [18] W. Sun, W. Jiang, G. Zhu, Y. Li, *J. Organomet. Chem.* **2018**, *873*, 91.
- [19] P. Kaur, B. Kumar, V. Kumar, R. Kumar, *Tetrahedron Lett.* **2018**, *59*, 1986.
- [20] A. Bukowska, W. Bukowski, K. Bester, K. Hus, *Appl. Organomet. Chem.* **2017**, *31*, e3847.

- [21] G. H. Dang, H. Q. Lam, A. T. Nguyen, D. T. Le, T. Truong, N. T. S. Phan, *J. Catal.* **2016**, 337, 167.
- [22] U. Chinna Rajesh, U. Gulati, D. S. Rawat, *ACS Sustainable Chem. Eng.* **2016**, 4, 3409.
- [23] X. Liu, B. Lin, Z. Zhang, H. Lei, Y. Li, *RSC Adv.* **2016**, 6, 94399.
- [24] M. Gholinejad, B. Karimi, A. Aminianfar, M. Khorasani, *ChemPlusChem* **2015**, 80, 1573.
- [25] X. Xiong, H. Chen, R. Zhu, *Cat. Com.* **2014**, 54, 94.
- [26] B. J. Borah, S. J. Borah, L. Saikia, D. K. Dutta, *Catal. Sci. Technol.* **2014**, 4, 1047.
- [27] M. Srinivas, P. Srinivasu, S. K. Bhargava, M. L. Kantam, *Catal. Today* **2013**, 208, 66.
- [28] J. Dulle, K. Thirunavukkarasu, M. C. Mittelmeijer-Hazeleger, D. V. Andreeva, N. R. Shiju, G. Rothenberg, *Green Chem.* **2013**, 15, 1238.
- [29] I. Luz, F. X. Llabrés i Xamena, A. Corma, *J. Catal.* **2012**, 285, 285.
- [30] M. J. Aliaga, D. J. Ramón, M. Yus, *Org. Biomol. Chem.* **2010**, 8, 43.
- [31] G. Shore, W. J. Yoo, C. J. Li, M. G. Organ, *Chem. – Eur. J.* **2010**, 16, 126.
- [32] M. Nasrollahzadeh, S. Mohammad Sajadi, A. Rostami-Vartooni, *J. Colloid Interface Sci.* **2015**, 459, 183.
- [33] S. Luo, J. Li, L. Zhang, H. Xu, J.-P. Cheng, *Chem. – Eur. J.* **2008**, 14, 1273.
- [34] P. Barbaro, *Chem. – Eur. J.* **2006**, 12, 5666.
- [35] T. Saegusa, A. Yamada, S. Kobayashi, S. Yamashita, *J. Appl. Polym. Sci.* **1979**, 23, 2343.
- [36] T. Li, Z. Wang, J. Yu, Y. Wang, J. Zhu, Z. Hu, *High Perform. Polym.* **2019**, 31, 1054.
- [37] X. Liang, S. Gao, G. Gong, Y. Wang, J.-G. Yang, *Catal. Lett.* **2008**, 124, 352.
- [38] F. Liu, L. Zhou, W. Wang, G. Yu, S. Deng, *Chemosphere* **2020**, 241, 125122.
- [39] C.-J. Yoo, P. Narayanan, C. W. Jones, *J. Mater. Chem. A* **2019**, 7, 19513.
- [40] R. P. Vasquez, *Surf. Sci. Spectra* **1998**, 5, 279.
- [41] Y. Yu, J. Chen, J. Wang, Y. Chen, *Chinese J. Catal.* **2016**, 37, 281.
- [42] S. H. Al-Harthi, M. Al-Barwani, M. Elzain, A. T. Al-Hinai, N. Al-Naamani, I. Al-Amri, T. Hysen, *Appl. Phys. A* **2011**, 105, 469.
- [43] B. Lindberg, R. Maripuu, K. Siegbahn, R. Larsson, C. G. Gölander, J. C. Eriksson, *J. Colloid Interface Sci.* **1983**, 95, 308.

SUPPORTING INFORMATION

Additional supporting information may be found online in the Supporting Information section at the end of this article.

How to cite this article: Jiang W, Xu J, Sun W, Li Y. CuSO₄ nanoparticles loaded onto poly (toluenesulfonic acid-formaldehyde)/polyethyleneimine composites: An efficient retrievable catalyst for A₃/decarboxylative A₃ reactions. *Appl Organomet Chem.* 2021;35:e6167. <https://doi.org/10.1002/aoc.6167>